Kim et al. Journal for ImmunoTherapy of Cancer (2019) 7:339
https://doi.org/10.1186/s40425-019-0785-8

Journal for ImmunoTherapy of Cancer

RESEARCH ARTICLE Open Access

Tumor microenvironment dictates regulatory T cell phenotype: Upregulated immune checkpoints reinforce suppressive function

Hye Ryun Kim[1†], Hyo Jin Park[2†], Jimin Son[2†], Jin Gu Lee[3], Kyung Young Chung[3], Nam Hoon Cho[4], Hyo Sup Shim[4], Seyeon Park[2], Gamin Kim[1], Hong In Yoon[5], Hyun Gyung Kim[6], Yong Woo Jung[6], Byoung Chul Cho[1], Seong Yong Park[3*], Sun Young Rha[1*] and Sang-Jun Ha[2*]

Abstract

Background: Regulatory T (T_{reg}) cells have an immunosuppressive function in cancer, but the underlying mechanism of immunosuppression in the tumor microenvironment (TME) is unclear.

Methods: We compared the phenotypes of T cell subsets, including T_{reg} cells, obtained from peripheral blood, malignant effusion, and tumors of 103 cancer patients. Our primary focus was on the expression of immune checkpoint (IC)-molecules, such as programmed death (PD)-1, T-cell immunoglobulin and mucin-domain containing (TIM)-3, T cell Ig and ITIM domain (TIGIT), and cytotoxic T lymphocyte antigen (CTLA)-4, on T_{reg} cells in paired lymphocytes from blood, peritumoral tissue, and tumors of 12 patients with lung cancer. To identify the immunosuppressive mechanisms acting on tumor-infiltrating T_{reg} cells, we conducted immunosuppressive functional assays in a mouse model.

Results: $CD8^+$, $CD4^+$ T cells, and T_{reg} cells exhibited a gradual upregulation of IC-molecules the closer they were to the tumor. Interestingly, PD-1 expression was more prominent in T_{reg} cells than in conventional T (T_{conv}) cells. In lung cancer patients, higher levels of IC-molecules were expressed on T_{reg} cells than on T_{conv} cells, and T_{reg} cells were also more enriched in the tumor than in the peri-tumor and blood. In a mouse lung cancer model, IC-molecules were also preferentially upregulated on T_{reg} cells, compared to T_{conv} cells. PD-1 showed the greatest increase on most cell types, especially T_{reg} cells, and this increase occurred gradually over time after the cells entered the TME. PD-1 high-expressing tumor-infiltrating T_{reg} cells displayed potent suppressive activity, which could be partially inhibited with a blocking anti-PD-1 antibody.

Conclusions: We demonstrate that the TME confers a suppressive function on T_{reg} cells by upregulating IC-molecule expression. Targeting IC-molecules, including PD-1, on T_{reg} cells may be effective for cancer treatment.

Keywords: Tumor microenvironment, Regulatory T cells, Immune checkpoints, Programmed cell death 1 receptor

* Correspondence: syparkcs@yuhs.ac; rha7655@yuhs.ac; sjha@yonsei.ac.kr
†Hye Ryun Kim, Hyo Jin Park, Jimin Son contributed equally to this work and are joint first authors.
[3]Department of Thoracic and Cardiovascular Surgery, Yonsei University College of Medicine, 50 Yonsei-ro, Seodaemun-Gu, Seoul 120-752, South Korea
[1]Yonsei Cancer Center, Division of Medical Oncology, Yonsei University College of Medicine, 50 Yonsei-ro, Seodaemun-Gu, Seoul 120-752, South Korea
[2]Department of Biochemistry, College of Life Science & Biotechnology, Yonsei University, Seoul, South Korea
Full list of author information is available at the end of the article

Background

The recent development of immune checkpoint inhibitors (ICIs) has revolutionized cancer treatment. ICIs specific for anti-cytotoxic T lymphocyte antigen (CTLA)-4 or anti-programmed death (PD)-1 have improved patient survival and have been approved for the treatment of several cancer types, including non-small cell lung cancer (NSCLC), melanoma, head and neck cancer, bladder cancer, and renal cell cancer [1–3].

The tumor microenvironment (TME) and the immune system play critical roles in cancer progression and clinical outcome [4, 5]. Regulatory T (T_{reg}) cells are highly immunosuppressive and contribute to the maintenance of self-tolerance and immune homeostasis in humans [6, 7]. T_{reg} cells infiltrate tumors and promote their progression by suppressing antitumor immunity in the TME. Depleting T_{reg} cells can lead to spontaneous tumor regression due to enhanced antitumor response [7, 8]. Interaction of T_{reg} cells with TME enhances their immunosuppressive function and proliferative capacity. Several studies have shown that tumor-infiltrating T_{reg} cells are phenotypically distinct from those in peripheral blood (PB) and normal tissues [9, 10], suggesting that their immunosuppressive function depends on environmental factors.

T_{reg} cells suppressive functions are associated with the expression of several immune checkpoint molecules (ICs), such as PD-1, CTLA-4, T-cell immunoglobulin and mucin-domain containing-3 (TIM)-3, and T cell Ig and ITIM domain (TIGIT) [3, 6, 11–14]. CTLA-4 and TIGIT act as tumor suppressors and thus, modulate the immune response in the TME [6, 15, 16]. Although the PD-1/PD ligand (PD-L)1 interaction was shown to promote the conversion of conventional T (T_{conv}) cells into T_{reg} cells to maintain the latter's population [17–19], it remains controversial whether PD-1 expression by T_{reg} cells suppresses antigen-specific T cell immune responses [20–22].

Recent studies have reported that IC-molecules are upregulated on T_{reg} cells within the TME or upon chronic infection and that T_{reg} cells-mediated immunosuppression correlates with the expression of IC-molecules on these cells [6, 12]. The upregulation of these molecules has also been linked to tumor progression, as it likely reinforces the suppressive function of T_{reg} cells in the TME. We previously reported that an increased level of PD-1 on T_{reg} cells during chronic viral infection enhances $CD8^+$ T cell immune suppression via interaction with PD-L1 on $CD8^+$ T cells [12]. On the contrary, high PD-1 expression on T_{reg} cells indicates dysfunctional and exhausted IFN-γ-secreting T_{reg} cells that are enriched in tumor infiltrates and have possibly lost their suppressive function [23]. So far, the precise role of PD-1 in the function of tumor-infiltrating T_{reg} cells in the TME is controversial. Given the significance of PD-1 in modulating immune responses and its paradoxical role as both an activation and exhaustion marker, clarifying the function of PD-1-positive T_{reg} cells and their role in regulating anti-tumor immune responses is important [23].

To evaluate the suppressive function of tumor-infiltrating T_{reg} cells in the TME, we comprehensively compared the phenotypes of T cell subsets, including T_{reg} cells, obtained from PB, malignant effusion (ME), and tumor (TM) samples of patients with cancer. We also characterized T_{reg} cells in paired lymphocyte samples obtained from blood, peri-tumoral tissue, and tumors of patients with lung cancer. Using a lung cancer mouse model, we investigated the suppressive function and mechanism of action of tumor-infiltrating T_{reg} cells in the TME. We found that PD-1 was upregulated in tumor-infiltrating T_{reg} cells and played a role in suppressing $CD8^+$ T cell proliferation through PD-1/PD-L1 interactions. These results suggest that infiltrated PD-1-expressing T_{reg} cells in TME are a potential therapeutic target for anti-cancer treatment.

Methods

Study design

Patients with stage IV cancer with ME and patients with cancer who planned to undergo surgical resection between April 2012 and December 2017 at the Severance Hospital were prospectively enrolled. Inclusion criteria were as follows: 1) over 20 years old; 2) stage IV cancer with malignant pleural effusion or ascites confirmed by cytology, or cancer with scheduled surgery; and 3) written informed consent. We collected 300 cc of effusions and simultaneously obtained 10 cc of PB from patients with stage IV cancer with ME, if available. In patients who underwent surgery, we collected TM-adjacent normal tissue, and 10 cc of PB to isolate peripheral blood lymphocytes (PBLs). The study was approved by the Institutional Review Board of Severance Hospital. We categorized the samples into three groups: 1) PBLs, 2) ME from patients with stage IV cancer, and 3) TM from patients with cancer who underwent surgery. To analyze the characteristics of T_{reg} cells in TME, we also collected paired peritumoral tissue lymphocytes (pTILs), tumor-infiltrating lymphocytes (TILs), and PBLs at the same day from 12 patients with NSCLC who underwent curative resection.

Isolation of PB mononuclear cells and ME lymphocytes

PB mononuclear cells were isolated from 10 cc PB collected into EDTA tubes by separation over a Percoll (Sigma-Aldrich) gradient. Lymphocytes were isolated from 500 cc of ME by discontinuous density gradient centrifugation on Percoll. To isolate TILs, lung TMs

were chopped and then incubated with a solution containing 1 mg/mL collagenase type IV (Worthington Biochemical) and 0.01 mg/mL DNaseI (Sigma-Aldrich) at 37 °C for 25 min. TILs were isolated by Percoll gradient after washing dissociated tissues with ice-cold RPMI1640.

Flow cytometry and antibodies

Flow cytometry was performed using a FACS CANTOII (BD Biosciences, Franklin Lakes, NJ, USA) and CytoFLEX (Beckman Coulter, IN, USA). Data were analyzed using FlowJo software (Tree Star, OR, USA).

For immunolabeling of human samples, fluorophore-conjugated monoclonal antibodies against the following proteins were used: CD4 (RPA-T4), CD3 (OKT3), PD-1 (EH12.2H7), and CTLA-4 (BNI3) (all from Biolegend, San Diego, CA, USA); TIM-3 (344823) and TIGIT (741182) (both from R & D Systems, Minneapolis, MN, USA); CD25 (M-A251) (BD Biosciences, Franklin Lakes, NJ, USA); and Foxp3 (PCH101) (eBioscience, San Diego, CA, USA). The LIVE/DEAD Fixable Red Dead Cell Stain kit was from Invitrogen (Carlsbad, CA, USA). T_{reg} cells labeled with various antibodies (except for the antibody against Foxp3) were fixed and permeabilized with Foxp3 fixation/permeabilization solution (eBioscience). Foxp3 antibody was then administered for intracellular labeling of T_{reg} cells. The proportion of $CD4^+$ and $CD8^+$ T cells among total lymphocytes was determined, and the fraction of Foxp3-positive $CD4^+$ T cells was quantified.

For immunolabeling of mouse samples, fluorophore-conjugated monoclonal antibodies against the following proteins were used: CD4 (RM4–5), Ly5.1 (A20), PD-1 (29F.1A12), TIM-3 (RMT3–23), NK1.1 (PK136), and DX5 (DX5) (all from Biolegend); and CD8 (53-6.7), CD25 (PC61.5), CTLA-4 (UC10-4B9), TIGIT (G1GD7), and F4/80 (BM8) (all from eBioscience); and CD11b (M1/79) (BD Biosciences). The LIVE/DEAD Fixable Near-IR Dead Cell Stain kit was from Invitrogen. T_{reg} cells labeled with various antibodies (except for the antibodies against Foxp3 and CTLA-4) were fixed and permeabilized with Foxp3 fixation/permeabilization solution (eBioscience, San Diego, CA, USA). Foxp3 antibody was then administered for intracellular labeling of T_{reg} cells. The proportions of $CD4^+$ and $CD8^+$ T cells among lymphocytes were determined, and the fraction of Foxp3-positive $CD4^+$ T cells was quantified. To prevent myeloid cells from non-specific staining, samples were preincubated with anti-CD16/32 (93) (eBioscience) before immunolabeling with fluorophore-conjugated antibodies.

Mouse TM model and lymphocyte isolation

Female C57BL/6, C57BL/6-$Rag2^{-/-}$, and C57BL/6-Ly5.1 congenic mice (5–6 weeks) were purchased from Charles River Laboratories (Wilmington, MA, USA) and Jackson Laboratories (Bar Harbor, ME, USA). To generate lung TM bearing mice, 5×10^5 TC-1 cells were intravenously injected into C57BL/6 mice via the tail-vein. Mice were sacrificed on day 21 post-injection. Lymphocytes were isolated from the spleen, normal lung, and lung tumor as previously described [9]. The number of tumor nodules on left upper lobe of the lung was counted at day 12, 16, and 21 post-injection. All animal protocols were approved by the Institutional Animal Care and Use Committee of the Yonsei University Laboratory Animal Research Center (2013–0115).

In vitro suppression assay using mouse lymphocytes

For the T_{reg} cells suppression assay, $CD4^+CD25^+$ T_{reg} cells (10^5/well) were co-cultured with $CD8^+$ T cells (10^5/well) with Dynabeads mouse T-activator CD3/CD28 (Thermo Fisher Scientific, Waltham, MA, USA) in a 96-well U-bottom plate at 37 °C for 72 h. For the CellTrace Violet dilution assay, $CD8^+$ T cells were isolated from the spleen of naïve mice using a $CD8^+$ T Cell Isolation kit (Miltenyi Biotec, Bergisch Gladbach, Germany) and labeled with 5 μM CellTrace Violet (Thermo Fisher Scientific). $CD4^+CD25^+$ T_{reg} cells were separately isolated from the spleen and tumor of TM-bearing mice on day 21 post-injection using $CD4^+CD25^+$ Regulatory T Cell Isolation kit (Miltenyi Biotec, Bergisch Gladbach, Germany). To inhibit cell migration, Transwell membranes (0.4 mm pore; BD Biosciences) were inserted into 24-well plate. $CD4^+CD25^+$ T_{reg} cells (10^6/well) were co-cultured with $CD8^+$ T cells (10^6/well) with Dynabeads mouse T-activator CD3/CD28 (Thermo Fisher Scientific) in a 24-well plate at 37 °C for 72 h.

For PD-1 blockade in tumor-infiltrating T_{reg}, $CD4^+CD25^+$ T_{reg} cells (2.5×10^4/well) isolated from tumor lymphocytes of TM bearing mice on day 14 post-injection were preincubated with 10 μg/mL anti-PD-1 antibody (RMP1–14) or rat IgG2a isotype control (2A3) (Bio X Cell) at 4 °C for 1 h, washed twice, and then co-cultured with $CD8^+$ T cells (10^5/well) in the presence of mouse T-activator CD3/CD28 Dynabeads for 68 h.

Adoptive cell transfer for in vivo suppression assay

To examine the functionality of TIL T_{reg} ($PD\text{-}1^{hi}$) and spleen T_{reg} ($PD\text{-}1^{lo}$) cells, $CD4^+CD25^+$ T_{reg} cells were isolated from the tumor and spleen of TM bearing mice at day 21 post-injection using $CD4^+CD25^+$ Regulatory T Cell Isolation kit (Miltenyi Biotec). $Ly5.1^+$ $CD8^+$ T cells were isolated from naïve C57BL/6-Ly5.1 congenic mice. $Ly5.1^+$ $CD8^+$ T cells (2×10^6) were injected i.v. into recipient $Rag2^{-/-}$ mice alone or with $Ly5.2^+$ TIL T_{reg} or spleen T_{reg} (1×10^6). At day 7 after cell transfer, splenocytes isolated from $Rag2^{-/-}$ mice were analyzed for homeostatic expansion of the $Ly5.1^+$ $CD8^+$ T cell population using FACS.

In vitro suppression assay using human lymphocytes

$CD4^+CD25^+$ T_{reg} cells were isolated from the tumor tissue and peripheral blood of NSCLC patients, using human $CD4^+CD25^+CD127^{dim/-}$ Regulatory T Cells Isolation Kit II (Miltenyi Biotec, Bergisch Gladbach, Germany). $CD8^+$ T cells were isolated from the paired peripheral blood of NSCLC patients using human $CD8^+$ T Cell Isolation kit (Miltenyi Biotec, Bergisch Gladbach, Germany) and subsequently labeled with 5 μM CellTrace Violet. The $CD8^+$ T cells (10^5/well) were co-cultured with $CD4^+CD25^+$ T_{reg} cells (5×10^4/well) isolated from either tumor tissue or peripheral blood in the presence of 2.5 μl/well of Dynabeads human T-activator CD3/28 (Thermo Fisher Scientific) at 37 °C for 72 h.

Multi-color immunofluorescence analysis

For multicolor immunofluorescence analysis, lungs were isolated, fixed with 2% paraformaldehyde/phosphate buffered saline overnight at 4 °C, and then embedded in OCT compound (Sakura). Tissue blocks were frozen in 2-methyl butane and cooled on dry ice. Frozen blocks were cut to a thickness of 8 μm and mounted on the silane-coated slide. Sections were stained with 4,6-diamidino-2-phenylindole (DAPI; Invitrogen) and with antibodies for anti-CD8α (Clone 53–6.7), anti-CD4 (clone RM4–5), anti-CD279 (clone RMP1–30), and anti-GFP (clone 1GFP63) for amplification of Foxp3-GFP signals (Biolegend). Streptavidin-conjugated horseradish peroxidase was used for staining of biotin-conjugated antibodies, and TSA Cyanine 3 Tyramidetetramethylrhodamine reagent (SAT704A001EA; PerkinElmer) was subsequently added for amplification. Images was acquired using a microscope (Carl Zeiss Co. Ltd) and analyzed with ImageJ 1.50b software.

Statistical analysis

Data were analyzed using Prism 5.0 software (GraphPad Inc., CA, USA). The Student's *t*-test, one-way analysis of variance, and the least significant difference test were used, where appropriate, to evaluate the significance of differences among groups. All statistical analyses were conducted with a significance level of $\alpha = 0.05$ ($P < 0.05$).

Results

Patient characteristics

We enrolled 103 patients: 72 were stage IV cancer patients with ME, and 31 were patients with operable disease (not stage IV) who underwent surgical resection. Detailed information of the patients from which PB, ME, or TM were obtained is described in Additional file 6: Table S1. The total number of tumor specimens was divided into three groups based on the specimen type: PB, 20.7% (28/135); ME, 56.2% (76/135); and TM, 23.1% (31/135). Detailed analyses of immune subsets as well as the levels of their immune checkpoints were performed in PBLs (PB group), effusion-infiltrating lymphocytes (EILs) (ME group), and TILs (TM group). Primary cancer types in the ME group were NSCLC, 43.1% (31/72); gastric cancer, 22.2% (16/72); colon cancer, 5.6% (4/72), and breast cancer, 5.6% (4/72). The types of ME were ascites, 59.7% (43/76) and pleural effusion, 45.8% (33/76), with four patients having both (Additional file 6: Table S1). The presence of malignant cancer cells and TILs in TM or ME was pathologically or cytologically confirmed (Fig. 1a).

T_{conv} with exhausted phenotypes are abundant in TM and ME

To investigate T cell subsets in three different tumor specimens, we compared the ratio of $CD4^+$ and $CD8^+$ T cells in PBLs, EILs, and TILs isolated from PB, ME, and TM, respectively. The percentage of $CD4^+$ T cells was higher among TILs than among PBLs or EILs. In contrast, the percentage of $CD8^+$ T cells was markedly lower among TILs than among PBLs or EILs (Fig. 1b), suggesting that the migration of cytotoxic lymphocytes (CTLs) into the TM was inhibited.

The phenotypes of PBLs, EILs, and TILs were compared by quantifying $CD4^+$ and $CD8^+$ T cells expressing PD-1 and TIM-3. The percentage of PD-1- or TIM-3-expressing $CD4^+$ or $CD8^+$ T cells was the highest among TILs, with lower percentages in EILs and PBLs (Fig. 1c, d), suggesting that T cells derived from TM and ME show more pronounced T cell exhaustion than those derived from PBLs.

High expression of PD-1 in T_{reg} cells of ME and TM

We next examined how T_{reg} cells expressing forkhead box (Fox) p3 are distributed and differ phenotypically in PB, ME, and TMs. T_{reg} cells showed greater accumulation in TILs than in PBLs and EILs of patients or in PBLs of healthy controls (Fig. 2a). Interestingly, T_{reg} cells in TILs expressed a higher level of PD-1 than those in PBLs and EILs; moreover, the PD-1-expressing $Foxp3^+$ population among $CD4^+$ T cells was also larger in TILs than in EILs, which, in turn, had a larger population than PBLs (Fig. 2b). To further characterize $CD4^+$ T cells in different tissues, we compared PD-1 in $Foxp3^+$ and $Foxp3^-$ $CD4^+$ T cells (Fig. 2c). The proportion of PD-1-expressing cells in both $CD4^+$ cells was larger in EILs and TILs than in PBLs. These results indicate that PD-1 expression by T_{reg} cells and T_{conv} cells clearly reflect the TME, as PD-1 expression increased in the following order: TILs > EILs > PBLs.

We next investigated whether the characteristics of $CD4^+$ T cells, $CD8^+$ T cells, and T_{reg} cells were altered in MEs depending on the cancer type. As shown in Additional file 1: Figure S1, the abundance of these cells and their expression of PD-1 in MEs were comparable in

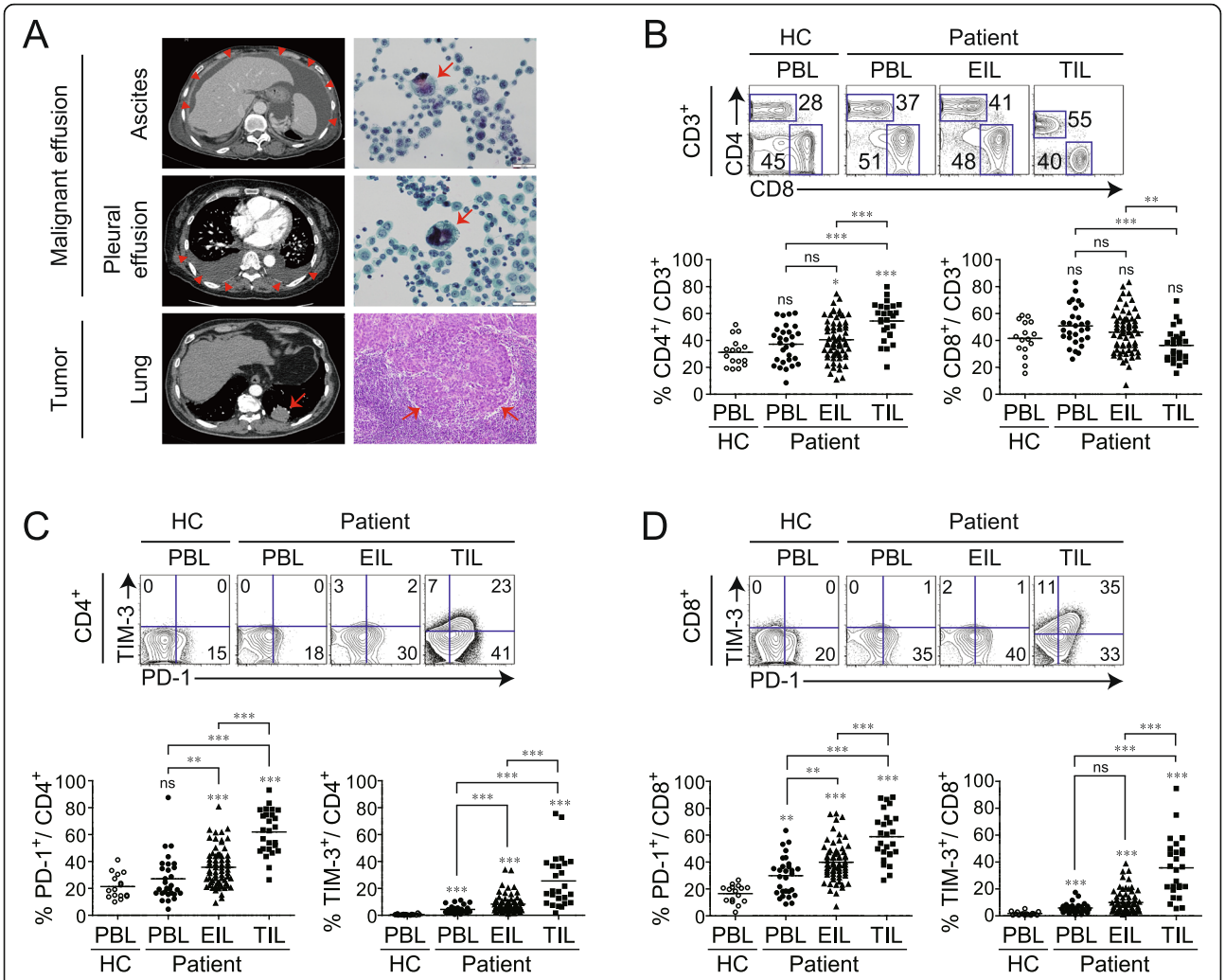

Fig. 1 T cell characteristics and PD-1 expression in T_{conv} of patients with cancer. Malignant effusions, such as ascites, and pleural effusions were extracted from patients with stage IV cancer. Tumor-infiltrating lymphocytes were obtained from the tumors of patients with non-small cell lung cancer (NSCLC) and colon cancer. **a** Left, computed tomography images showing malignant ascites (upper), pleural effusion (middle), and lung cancer lesions in left lower lobe (bottom) of a patient with NSCLC. Right, cytological analysis of malignant effusion and histological analysis of lung cancer tissue. Red arrows indicate malignant effusion and cancer (left column) and tumor cells (right column). **b** Proportions of $CD4^+$ and $CD8^+$ T cells among $CD3^+$ T cells. Representative plots (upper) and statistics (bottom) are shown. **c**, **d** PD-1 and TIM-3 expression on $CD4^+$ and $CD8^+$ T cells. Representative plots of PD-1 and TIM-3 expression (upper) and percentages of total PD-1^+ (bottom left) and TIM-3^+ (bottom right) cells among $CD4^+$ and $CD8^+$ T cells are shown. Peripheral blood lymphocytes (PBLs), effusion-infiltrating lymphocytes (EILs), and tumor-infiltrating lymphocytes (TILs) were isolated from healthy control donors (HC) and patients with cancer (PBLs of HC, $n = 16$; PBLs, $n = 28$; EILs, $n = 76$; TILs, $n = 31$). Lines in the scatterplot represent the mean values. ns, not significant; $^*P < 0.05$, $^{**}P < 0.01$, $^{***}P < 0.001$ (Mann-Whitney test)

different types of cancer, although it is worth noting that there were more T_{reg} cells than there were $CD4^+$ or $CD8^+$ T_{conv} cells expressing PD-1. Interestingly, the degree of infiltration of PD-1^+ T_{reg} cells did not differ among ME samples derived from the different types of cancer, indicating that the presence of PD-1^+ T_{reg} cells in ME is a common feature across cancers of distinct histological origin (Additional file 1: Figure S1). Additionally, we compared the phenotype of T_{reg} between ascites and pleural effusion. As shown in Additional file 2: Figure S2, significant differences of the percentages of Foxp3^+ T_{reg} and PD-1^+ Foxp3^+ T_{reg} cells were not observed between ascites and pleural effusion. Moreover, the ascites and pleural effusions had a similar expression rate of PD-1 in Foxp3^+ T_{reg} and Foxp3^- T_{conv} cells.

Tumor-infiltrating T_{reg} are abundant in patients with lung cancer and express multiple IC-molecules

To clarify the characteristics of T_{reg} cells in the TME, we compared the frequency of T_{reg} cells and the expression of IC-molecules such as PD-1, TIM-3, TIGIT, and CTLA-4 in paired sets of tissue-derived lymphocytes, such as PBLs, pTILs, and TILs collected from 12 patients with NSCLC. As expected, T_{reg} cells were

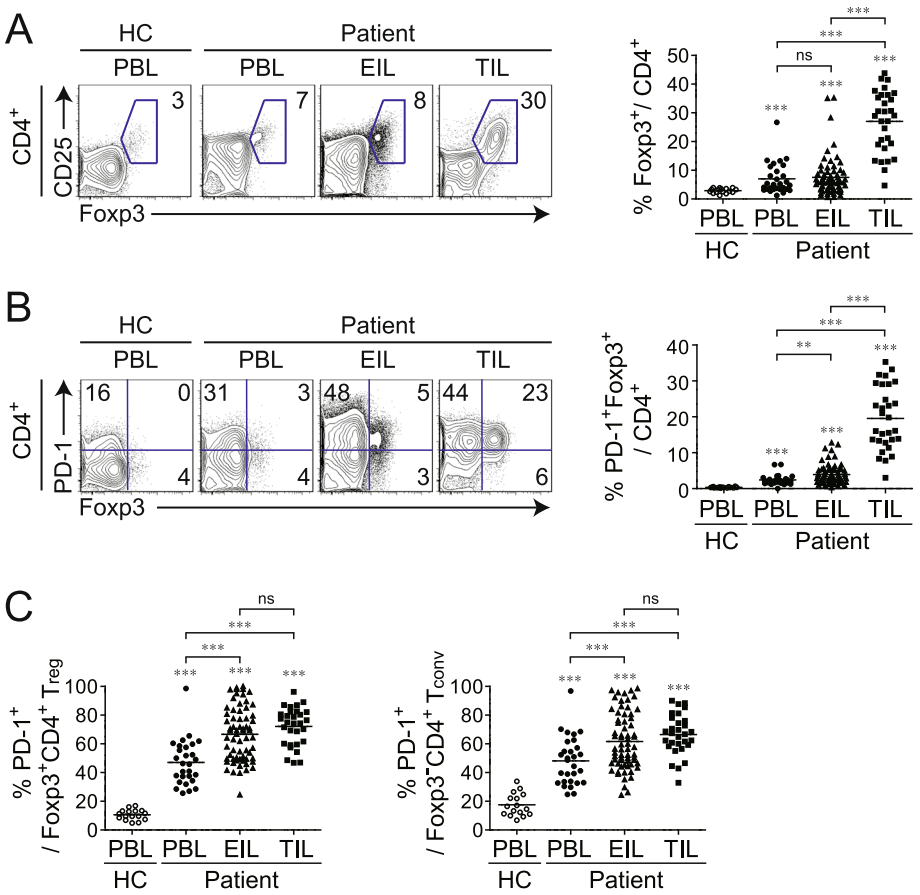

Fig. 2 PD-1 expression in Foxp3$^+$ T_{reg} in different tissue types of patients with cancer. **a** Representative plots of CD25 and Foxp3 expression (left) and proportion of Foxp3$^+$ T cells (right) among CD4$^+$ T cells. **b** Representative plots of PD-1 and Foxp3 expression (left) and proportion of PD-1 and Foxp3 co-expressing cells among total CD4$^+$ T cells (right). **c** Summary of PD-1-positive fraction of Foxp3$^+$ T_{conv} (left) and Foxp3$^-$ T_{reg} (right) cell populations among CD4$^+$ T cells. Peripheral blood lymphocytes (PBLs), effusion-infiltrating lymphocytes (EILs), and tumor-infiltrating lymphocytes (TILs) were isolated from healthy control donors (PBL, $n = 16$) and patients with cancer (PBL, $n = 28$; EIL, n = 76; TIL, $n = 31$). Lines in the scatterplot represent the mean values. ns, not significant; $^{**}P < 0.01$, $^{***}P < 0.001$ (Mann-Whitney test)

more highly enriched in TILs than in pTILs and PBLs (Fig. 3a). Moreover, more T_{reg}-expressing ICs were found among TILs than among pTILs and PBLs (Fig. 3b).

We also compared IC-molecule expression on different tumor-infiltrating T cell subsets. Among four different IC-molecules, PD-1 most clearly distinguished TME in all T cell subsets, because a significant increase in the PD-1$^+$ population was observed in the following order TIL > pTIL > PBL (Fig. 3c). Notably, PD-1 was higher in tumor-infiltrating Foxp3$^+$$T_{reg}$ cells (~ 98%) than in Foxp3$^-$$T_{conv}$ cells (~ 82%) or CD8$^+$ T_{conv} cells (78%). Furthermore, the number of PD-1-expressing tumor-infiltrating Foxp3$^+$ T_{reg} cells was greater than the number of tumor-infiltrating Foxp3$^+$ T_{reg} cells expressing other IC-molecules. It is therefore conceivable that PD-1 expression on T_{reg} cells is a TME marker. Additionally, we performed the in vitro suppressive assay using isolated CD4$^+$CD25$^+$ T_{reg} cells from the peripheral blood and tumor tissue of NSCLC patients and isolated CD8$^+$ T cells from the peripheral blood. Each tumor-infiltrating T_{reg} cells or peripheral T_{reg} cells was co-cultured with peripheral CD8$^+$ T cells with αCD3/CD28 stimulation. CD8$^+$ T cells proliferated at a high rate in the absence of T_{reg} cells and were more potently inhibited by PD-1^{hi} tumor-infiltrating T_{reg} cells than by PD-1^{lo} PBMC T_{reg} cells (Fig. 3d).

T_{reg} numbers and the expression of IC-molecules are altered during cancer progression in a mouse model

We previously showed that immune-exhaustion markers were highly expressed in tumor-infiltrating T_{reg} cells of patients with NSCLC. We therefore investigated the T_{reg} phenotype in greater detail in different tissues, using a mouse lung cancer model. We compared the expression levels of IC-molecules, such as PD-1, TIM-3, and TIGIT, on CD4$^+$ and CD8$^+$ T cells in different tissues from naïve and TM-bearing mice. As in patients with cancer

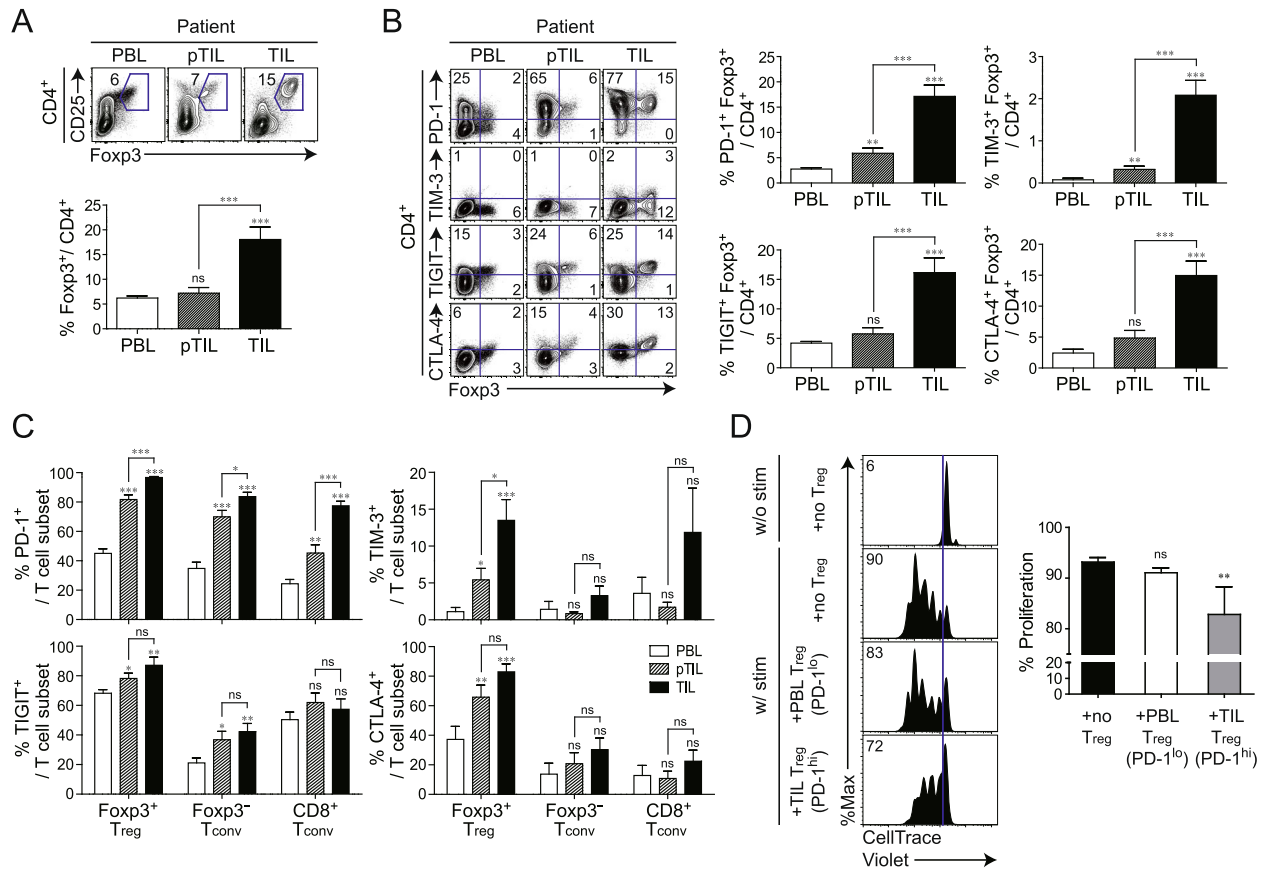

Fig. 3 PD-1-expressing tumor-infiltrating T_{reg} and their activated phenotype in patients with non-small cell lung cancer (NSCLC). **a** CD25 and Foxp3 expression in $CD4^+$ T cells (upper) and proportion of $Foxp3^+$ cells among total $CD4^+$ T cells (lower) in peripheral blood lymphocytes (PBLs), peritumoral infiltrating lymphocytes (pTILs), and tumor-infiltrating lymphocytes (TILs) derived from patients with NSCLC. **b** Representative plots of PD-1, TIM-3, TIGIT, CTLA-4, and Foxp3 expression in $CD4^+$ T cells (left) and percentage of $CD4^+$ T cells co-expressing PD-1, TIM-3, TIGIT, CTLA-4, and Foxp3 (right). **c** PD-1, TIM-3, TIGIT, and CTLA-4 expression in $Foxp3^+$ T_{reg}, $Foxp3^-$ T_{conv} and $CD8^+$ T_{conv} of these patients. **d** Enhanced suppression of $CD8^+$ T cells by PD-1-expressing tumor-infiltrating T_{reg} from NSCLC patients. T_{reg} were isolated from the peripheral blood and tumor tissue from NSCLC patients. Peripheral blood T_{reg} and tumor-infiltrating T_{reg} expressed low and high levels of PD-1, respectively. CellTrace Violet (CTV)-labeled $CD8^+$ T cells were stimulated in vitro with CD3/CD28 Dynabeads for 96 h in the absence or presence of each T_{reg} population. CTV dilution in proliferating $CD8^+$ T cells is indicated in each histogram. Histograms represent the percentages of proliferating cells. Lines in the bar graph represent the mean and mean ± SEM, respectively. ns, not significant; $^{**}P < 0.01$, $^{***}P < 0.001$ (Mann-Whitney test)

tissue, the expression of IC-molecules in $CD4^+$ and $CD8^+$ T cells was much higher in lung TM than in PB or spleen (Fig. 4a, b). Among the populations expressing IC-molecules, PD-1-expressing $CD4^+$ and $CD8^+$ T cells were more abundant in the TM.

We next examined whether IC-molecules are preferentially upregulated on T_{reg} cells (compared to T_{conv}) in TM, as was observed in patient tissues. PB, spleen, and lung lymphocytes were isolated at different time points after TC-1 injection (Fig. 5a). Starting at 12 days after TC-1 injection, an increase in the number of $Foxp3^+$ T_{reg} cells was observed in TM and the T_{reg} cells fraction reached 20% of total $CD4^+$ T cells, a nearly 3-fold increase compared to that in the non-TM lung (Fig. 5b). At 3 weeks after TC-1 injection, $Foxp3^+$ T_{reg} cells were more abundant in the TM than in the PB or spleen (Fig. 5c). $Foxp3^+$ T_{reg} cells in TM showed significant increases in PD-1, TIM-3, TIGIT, and CTLA-4, compared to other tissues (Fig. 5d). Moreover, tumor-infiltrating T_{reg} cells expressed much higher levels of IC-molecules than tumor-infiltrating T_{conv} (Fig. 5e). Most T_{reg} cells (~ 80%), but only a low frequency of T_{conv} (~ 20%) expressed PD-1 in TM. PD-1 was markedly upregulated 21 days after TC-1 injection, and the same trend was observed for TIM-3 and TIGIT, although the increases in the levels of these molecules were less prominent (Fig. 5f). Unlike PD-1, TIM-3, and TIGIT, CTLA-4 was already upregulated in T_{reg} cells before TC-1 injection and its expression progressively increased over time (Fig. 5f). Thus, expression of IC-molecules, especially PD-1, on T_{reg} cells increases

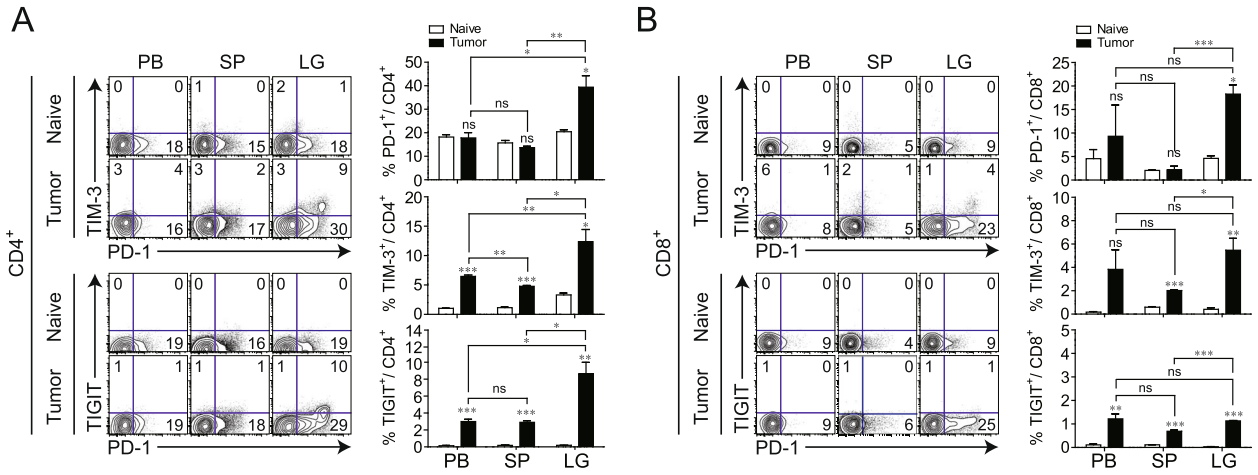

Fig. 4 Differential expression of immune checkpoint (IC) molecules on $CD4^+$ and $CD8^+$ T cells in mice with lung cancer. To induce lung adenocarcinoma, TC-1 cells were intravenously injected into syngeneic mice. **a**, **b** Tumor-bearing mice at 3 weeks after TC-1 cell injection and naïve control mice were sacrificed, and lymphocytes were isolated from peripheral blood (PB), spleen (SP), and lung (LG). (Left) Expression levels of PD-1, TIM-3, and TIGIT on $CD4^+$ and $CD8^+$ T cells were assessed. (Right) Summary of the proportions of IC molecules expressed on populations of $CD4^+$ and $CD8^+$ T cells in PB, SP, and LG at the tumor site. Numbers in the plot indicate percentages of the corresponding population. Data are representative of three independent experiments ($n = 5$ mice per group in each experiment). ns, not significant; $^*P < 0.05$, $^{**}P < 0.01$, $^{***}P < 0.001$ (Student's *t*-test). The symbol above each column is the *P* value obtained when SP samples were compared to the corresponding samples from naïve mice (control)

with TM progression. As tumor numbers increased, immune checkpoints including PD-1, TIM-3, TIGIT, and CTLA-4 increased (Additional file 3: Figure S3).

Immunosuppressive function of tumor-infiltrating T_{reg} in $CD8^+$ T cell response is mediated by PD-1/PD-L1 interaction

Among all IC-molecules examined, PD-1 was most highly upregulated in tumor-infiltrating T_{reg} cells. To determine the role of PD-1 on tumor-infiltrating T_{reg} cells, in the regulation of the $CD8^+$ T cell response, we compared the suppressive activity of T_{reg} expressing high- and low-levels of PD-1 (PD-1^{hi} T_{reg} cells from lung TM 3 weeks after TC-1 injection vs. PD-1^{lo} T_{reg} cells from the spleen of the same TM-bearing mice). $CD4^+CD25^+$ T_{reg} cells, isolated using a microbead-based Treg isolation kit ($CD4^+CD25^+$ Regulatory T Cell Isolation kit), was confirmed to be ~ 90% purified $Foxp3^+$ T_{reg} cells (Additional file 4: Figure S4). Each population was co-cultured with naïve $CD8^+$ cells with or without stimulation by αCD3/CD28. $CD8^+$ T cells proliferated at a high rate in the absence of T_{reg} cells and were more potently inhibited by PD-1^{hi} tumor-infiltrating T_{reg} cells than by PD-1^{lo}spleen T_{reg} cells (Fig. 6a). Similarly, interferon (IFN)-γ production was also more strongly suppressed by PD-1^{hi} tumor-infiltrating T_{reg} than by PD-1^{lo} spleen T_{reg} cells.

To investigate the role of PD-1 upregulation, induced by tumor-infiltrating T_{reg} cells, we examined whether the interaction between PD-1 on tumor-infiltrating T_{reg} cells and PD-L1 on $CD8^+$ T cells is required for immunosuppression in patients with cancer. PD-1 on tumor-infiltrating T_{reg} cells was blocked by incubation with an anti-PD-1 antibody. Unbound antibody was subsequently removed and the cells were co-cultured with $CD8^+$ T cells. We prepared T_{reg} cells, expressing an intermediate level of PD-1 that were isolated from lung TM in 2- rather than in 3-weeks after injection because T_{reg} cells, highly expressing PD-1, isolated at later timepoints, also co-expressed other IC-molecules (Fig. 5), making it difficult to differentiate the role of PD-1 in the suppressive function of T_{reg} cells from that of others.

Additionally, to clarify whether the potent suppressive function of PD-1^{hi} tumor-infiltrating T_{reg} cells is mediated via cell-to-cell contact between T_{reg} and $CD8^+$ cells or soluble factors produced from T_{reg} cells, we conducted the experiments with transwell membrane system to block cell migration (Fig. 6b). Transwell membranes were inserted into 24-well plate. CTV labeled $CD8^+$ T cells and $CD4^+CD25^+$ T_{reg} were placed into lower and upper wells, respectively, and αCD3/CD28 was added into both wells for stimulation. Suppression of T cell proliferation was not observed in the presence of the Transwell membrane. This data demonstrated that the suppression of $CD8^+$ T cell proliferation by T_{reg} requires cell to cell contact between each cell population (Fig. 6b). Next, we performed the in vivo experiment with TIL T_{reg} and spleen T_{reg} cellsalong with $Ly5.1^+CD8^+$ T cells. In line with in vitro data, when TIL T_{reg} cells was injected, $CD8^+$ T cell proliferation was significantly

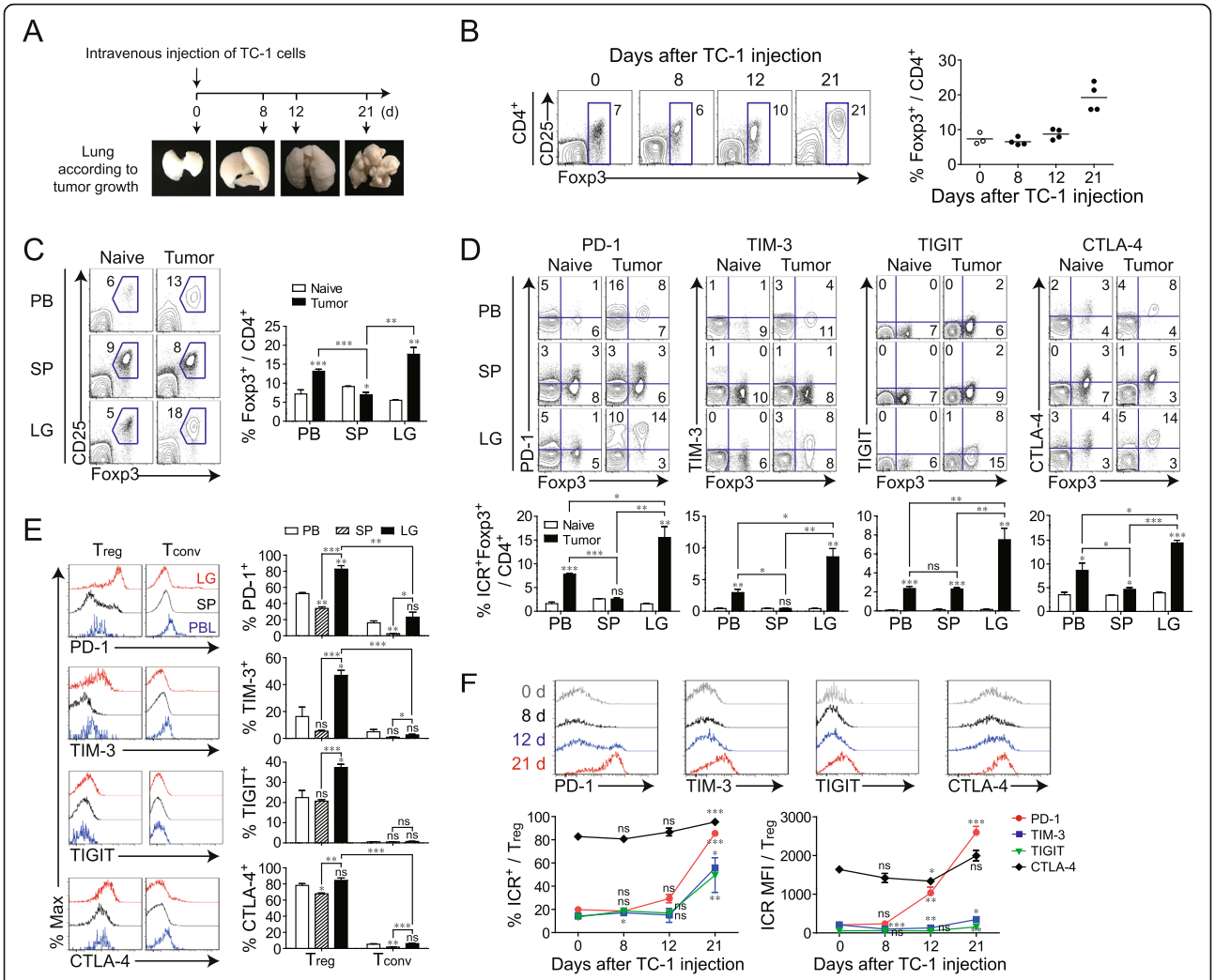

Fig. 5 Spatial and temporal dynamics of immune checkpoint (IC) molecule expression on T_{reg} during cancer progression. **a** Schedule for establishing the TC-1 lung adenocarcinoma model and tumor formation at each time point. **b** Representative plots showing CD25 and Foxp3 expression in $CD4^+$ T cells (left) and changes at different time points after TC-1 TM tumor cell injection (right). **c** Representative plots of T_{reg} (left) and summary of the proportion of $Foxp3^+$ cells among $CD4^+$ T cells (right) in peripheral blood (PB), spleen (SP), and lung (LG). **d** Levels of PD-1, TIM-3, TIGIT, and CTLA-4 expression on $Foxp3^+CD4^+$ T_{reg} in PB, SP, and LG. **e** Levels of PD-1, TIM-3, TIGIT, and CTLA-4 expression on T_{reg} and T_{conv} in different tissues (PB, SP, and LG). **f** Changes in the levels of PD-1, TIM-3, TIGIT, and CTLA-4 expression on T_{reg} at different time points. Data are representative of three independent experiments ($n = 5$ mice per group in each experiment). ns, not significant; $^*P < 0.05$, $^{**}P < 0.01$, $^{***}P < 0.001$ (Student's *t*-test)

inhibited compared with spleen T_{reg} and no T_{reg} cells (Fig. 6c).

As shown in Fig. 6d, tumor-infiltrating T_{reg} cells that had been blocked with anti-PD-1 antibody, were significantly impaired in their ability to suppress the proliferation of $CD8^+$ T cells and IFN-γ production as compared to isotype antibody-treated tumor-infiltrating T_{reg} cells. Given that both mouse and human $CD8^+$ T cells can upregulate low affinity Fc receptors following activation [24, 25], we tested whether $CD8^+$ T cells upregulate Fc receptors in our system. We obtained splenocytes of TC-1 tumor bearing mice. We stained splenocytes with CD8, CD44, CD16/32 (FcγRIII/II), and CellTrace Violet and compared the expression of Fc receptor between with and without stimulation. Significant differences of CD16/32 were not observed between groups with and without stimulation (Additional file 5: Figure S5A). To validate the CD16/32 antibody, we analyzed the expression of CD16/32 on NK cells and macrophages. This antibody can specifically detect CD16/32 on these cells, so we excluded the possibility that no detection of CD16/32 on $CD8^+$ T cells after stimulation could be a problem of CD16/32 antibody (Additional file 5: Figure S5B). Taken together, our data demonstrated that the effect of anti-PD-1 is direct effect by

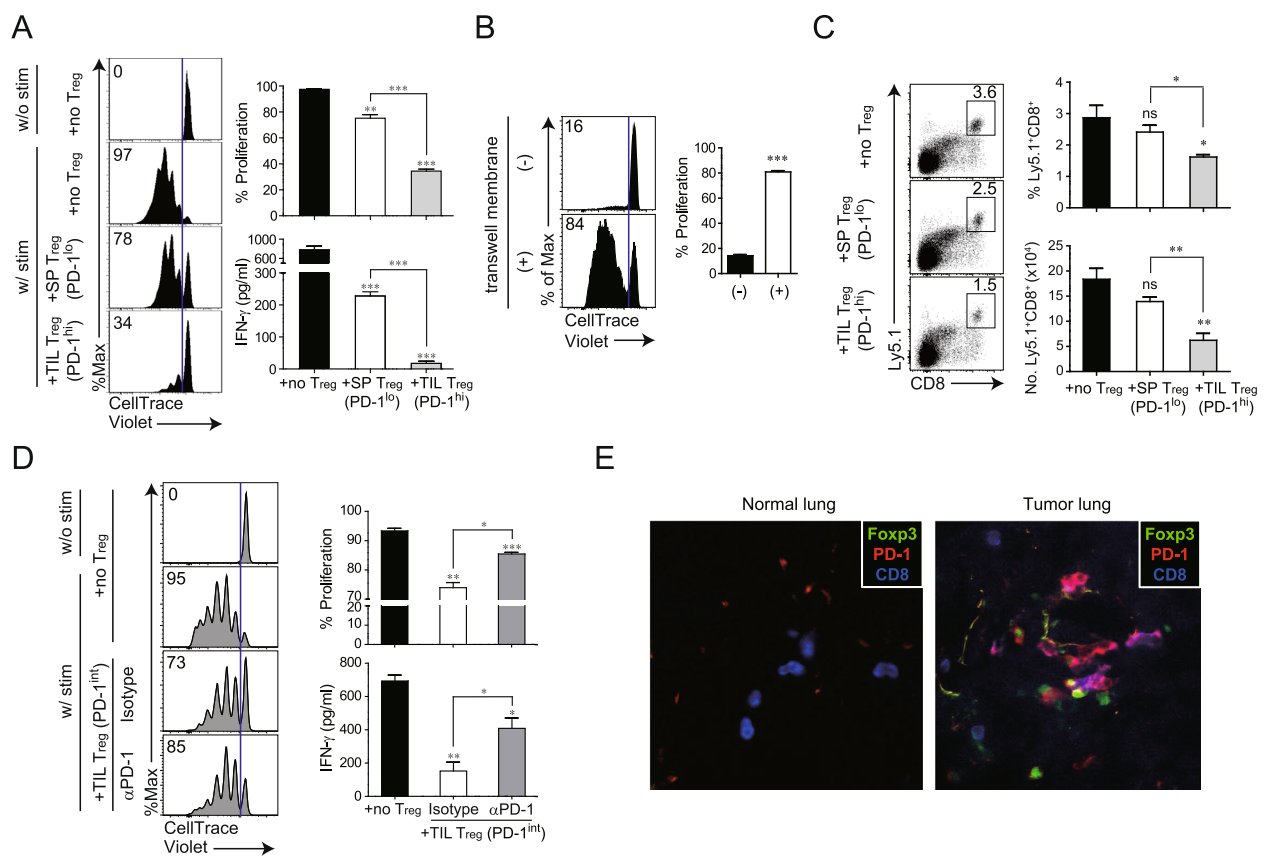

Fig. 6 Enhanced suppressive function of PD-1-expressing tumor-infiltrating T_{reg}. **a** Enhanced suppression of $CD8^+$ T cells by PD-1-expressing tumor-infiltrating T_{reg}. At 3 weeks after intravenous injection of TC-1 cells, T_{reg} were isolated from the spleen (SP) and lung of mice with TC-1 cell-induced tumors. SP T_{reg} and tumor-infiltrating T_{reg} expressed low and high levels of PD-1, respectively. CellTrace Violet (CTV)-labeled $CD8^+$ T cells were stimulated in vitro with CD3/CD28 Dynabeads for 72 h in the absence or presence of each T_{reg} population. CTV dilution in proliferating $CD8^+$ T cells is indicated in each histogram. Histograms represent the percentages of proliferating (upper) and IFN-γ-producing (lower) cells. **b** Contact-dependent T_{reg}-mediated suppression of $CD8^+$ T proliferation. CTV-labeled $CD8^+$ T cells were stimulated in vitro with CD3/CD28 Dynabeads and cocultured with tumor-infiltrating T_{reg} for 72 h in the absence or presence of a transwell membrane. **c** Homeostatic proliferation of donor $Ly5.1^+CD8^+$ T cells in the spleen isolated from $Rag2^{-/-}$ mice at 7 d after adoptive cell transfer. Representative plot (left) and absolute number (right) of donor $Ly5.1^+CD8^+$ T cells in the spleen. **d** PD-1-mediated suppressive activity of tumor-infiltrating T_{reg} isolated from the lungs of tumor-bearing mice 2 weeks after intravenous injection of TC-1 cells. At this time point, T_{reg} expressed intermediate levels of PD-1. CTV-labeled $CD8^+$ T cells were stimulated as shown in (**a**). Before co-culture of $CD8^+$ T cells with tumor-infiltrating T_{reg}, the latter were pre-incubated with an anti-PD-1 antibody or its isotype as control. CTV dilution in proliferating $CD8^+$ T cells is shown in the histograms, which represent the percentages of proliferating (upper) and IFN-γ-producing (lower) cells. (**e**) Representative immunofluorescence images of mouse lung tumor samples. Antibodies against Foxp3, CD8, and PD-1 were used to label and examine the interaction between T_{reg} and $CD8^+$ T cells expressing PD-1. Data are representative of two independent experiments. $^*P < 0.05$, $^{**}P < 0.01$, $^{***}P < 0.001$ (Student's *t*-test)

blocking of PD-1 pathway signaling rather than the effect of anti-PD-1 antibody mediated by ADCC.

A multi-color immunofluorescence analysis revealed that CD8, PD-1, and Foxp3 were co-localized in mouse tumor tissues (Fig. 6e), implying that $CD8^+$ cells and $Foxp3^+$ T_{reg} cells spatially interact in the TME.

Discussion

In this study, we examined the phenotype and function of T_{reg} cells as well as $CD4^+$ and $CD8^+$ T_{conv} cells that infiltrated into the TME, including the ME and TM from patients with cancer. We also investigated the mechanism by which T_{reg} cells induce immunosuppression using a mouse lung cancer model. Most tumor-infiltrating T_{reg} cells showed higher PD-1 expression than T_{conv} cells, implying that PD-1-expressing T_{reg} cells are a biological marker of the TME. Indeed, in T_{reg} cells derived from TMs of patients with NSCLC, PD-1 was the most clearly up-regulated IC-molecule. As previously reported, these cells exhibited an enhanced immunosuppressive function that was correlated with the extent of PD-1 up-regulation [12]. We speculate that PD-1-expressing tumor-infiltrating T_{reg} cells induce immunosuppression through the interaction of PD-1 and PD-L1, which may contribute to immune escape in TME.

Clarifying the link between this phenotype and enhanced suppressive function of tumor-infiltrating T_{reg} cells can provide insight into their suppressive mechanism in patients with cancer.

The predominant function of PD-1 in T_{reg} cells seems to be similar to that of CTLA-4; both proteins contribute to the maintenance of T_{reg} immunosuppressive function [15]. However, PD-1 expression on T_{reg} cells differed by cell location. For instance, PD-1 was expressed by T_{reg} cells in TMs but not in normal tissue or PBLs as depicted in Fig. 3. In contrast, T_{reg} cells had high basal CTLA-4 levels irrespective of the tissue of origin. This supports our assertion that PD-1 on T_{reg} cells is a more useful marker for characterizing the TME. We also examined whether the upregulation of PD-1 on tumor-infiltrating T_{reg} cells can reinforce their basal immune-suppressive function. High PD-1 expression in T_{reg} cells was associated with the suppression of $CD8^+$ T cells and PD-1 blockade abrogated the immune-suppressive function of T_{reg} cells, suggesting that an interaction between PD-1 on T_{reg} cells and PD-L1 expressed by another cell type—likely $CD8^+$ T cells [26]—is necessary for immunosuppression. Thus, elevated PD-1 expression on T_{reg} cells is a potential marker for immune escape in patients with cancer. These findings were consistent with our previously reported data that PD-1 upregulation in T_{reg} cells and the interaction between PD-1 on T_{reg} cells and PD-L1 expressed by effector T cells enhanced T cell-mediated immune suppression during chronic viral infection [12]. Thus, an immunotherapy targeting T_{reg} and PD-1 could be highly effective in patients with cancer.

We also investigated tumor-infiltrating T_{reg} and T_{conv} cells obtained from ME of patients with stage IV cancer. Most of the earlier studies of TME T_{reg} cells were performed in mice and focused on T_{reg} cells phenotype. Studies in patients with stage IV cancer have been hampered by the difficulty of obtaining sufficient TMs for analysis of T cell populations. To overcome this limitation, we developed an experimental model using ME from human patients with stage IV cancer as representative TME of stage IV cancer. This model will allow future examinations of various mechanistic aspects of human cancer through functional assays.

Several studies have reported IC expression on intratumoral T_{reg} cells and suggested potential roles of these ICs in the regulation of the immune response in mice [6, 15, 27]. We also showed here that ICs other than PD-1 were upregulated in T_{reg} cells. Studies on the relative contributions of these IC-molecules to immunosuppression in the TME may lead to the development more effective immunotherapies.

Regarding other PD-1-expressing immune cells than $CD8^+$ T cells and T_{reg} cells in TME and their role, Irving et al. reported that tumor-associated macrophages (TAMs) expressed PD-1 and PD-1-expressing TAMs increased over time in mouse model and progressive disease in human cancers [28]. PD-1 expressed on TAMs reduced their phagocytic potency against tumor cells and blockade of PD-1 pathway restored the macrophage phagocytosis, resulting in enhancing anti-tumor activity of TAMs. This data suggests that PD-1 expressed by TAMs is one of the mechanism for immune evasion. PD-1 expression was also described on NK cells in many different types of human and mouse cancers, where the PD-1 expressed by NK cells negatively regulated NK cell function even though its molecular mechanisms are not clearly demonstrated to date [29–34]. In addition, PD-1 has been reported to be expressed on innate lymphoid cells (ILCs), prevalently ILCs type 3 (ILC3s), as well as NK cells in pleural effusion of primary and metastatic tumors, albeit the role of PD-1 on ILC3s was not addressed [35].

Based on these reports, it is plausible that PD-1 expressed by different types of immune cells including CD8+ T cells, T_{reg} cells, NK cells, and ILCs in the TME probably contributes to immune evasion, leading to promotion of tumor cells. However, it has not been addressed yet which types of PD-1-expressing immune cells are most effectively involved in the PD-1-mediated immunosuppression. In addition, to compare the immunosuppressive activity of each immune cell subset, the level of PD-1 expression on each type of cells should be examined. In this regard, further study is needed to determine whether other PD-1-expressing immune cells than T_{reg} cells in the TME compensate for a lack of T_{reg} cells and which types of PD-1-expressing immune cells mostly impact on immune suppression in the TME.

T_{reg} cells expansion in the TME is widely recognized as an obstacle to successful immunotherapy in patients with cancer [5]. Previously, we demonstrated that T_{reg} cells depletion using an anti-CD25 antibody increased the abundance of functional antigen-specific $CD8^+$ T cells during chronic viral infection [12]. Furthermore, treatment with a neutralizing antibody also caused the elimination of non-T_{reg} and rapid replenishment of T_{reg} cells [36]. Thus, functional inactivation of T_{reg} cells and rejuvenation of exhausted T cells by targeting overexpressed PD-1 combined with temporal depletion of T_{reg} cells expressing IC-molecules may be a promising strategy to limit cancer progression.

Conclusions

In conclusion, our study provides insights into T_{reg} cells function and their suppressive mechanism in patients with cancer. We showed that the suppressive function of tumor-infiltrating T_{reg} cells was enhanced by the increase in their relative proportion and by the upregulation of the expression of inhibitory receptors, such as PD-1, TIM-3, and CTLA-4.

Supplementary information

Supplementary information accompanies this paper at https://doi.org/10.1186/s40425-019-0785-8.

Additional file 1: Figure S1. PD-1 expression on $CD4^+$, $CD8^+$, or T_{reg} in malignant effusion according to the different types of cancer patients including lung cancer, gastric cancer, breast cancer, and others.

Additional file 2: Figure S2. Comparison of T_{reg} phenotype between ascites and pleural effusion. (A) Percentage of Foxp3 in total $CD4^+$ T cells between ascites and pleural effusion (B) Percentage of PD-1^+Foxp3^+ in total $CD4^+$ T cells between ascites and pleural effusion (C) Percentage of PD-1^+ in Foxp3^+CD4 T_{reg} between ascites and pleural effusion (Left), percentage of PD-1^+in Foxp3^- CD4 T cells between ascites and pleural effusion.

Additional file 3: Figure S3. Correlation of the immune checkpoint including PD-1, TIM-3, TIGIT and CTLA4 expressed on T_{reg} as tumor nodule number increased. (A) PD-1, (B) TIM-3, (C) TIGIT, and (D) CTLA-4 expression on T_{reg} according to the increased tumor nodules. The number of tumor nodules was measured at day 12, 16, and 21 post-injection (n = 4–7 mice per group). Data are representative of two independent experiments. *$P < 0.05$, **$P < 0.01$, ***$P < 0.001$ (Student's t-test).

Additional file 4: Figure S4. Purification of tumor-infiltrating T_{reg} using microbead-based Treg isolation kit. T_{reg} were separately isolated from the spleen and from TM-bearing mice using a $CD4^+CD25^+$ Regulatory T Cell Isolation kit for suppressive function analysis. T_{reg}, isolated using a microbead-based Treg isolation kit, demonstrated ~ 90% purified Foxp3^+ T_{reg} compared with the 16% prior to isolation.

Additional file 5: Figure S5. Expression of CD16/32 on $CD8^+$ T cells after in vitro TCR activation and NK cells and macrophages. (A) The expression of CD16/32 on purified $CD8^+$ T cells activated by CD3/28 Dynabeads for 3 d. (B) The expression of CD16/32 on Dx5^+NK1.1^+ NK cells and CD11b^+F4/80^+ macrophages isolated from the spleen of naïve mouse.

Additional file 6: Table S1. Baseline characteristics of patients and specimens.

Acknowledgements
Not applicable.

Declarations
This manuscript has not been published or presented elsewhere in part or in entirety and is not under consideration by another journal. All study participants provided informed consent, and the study design was approved by the appropriate ethics review board. We have read and understood your journal's policies, and we believe that neither the manuscript nor the study violates any of these. There are no conflicts of interest to declare. The author contributions are described below.

Authors' contributions
Conception and design: HRK, SYP, SYR, S-JH. Financial support: HRK, S-JH. Administrative support: HRK, SYP, SYR, S-JH. Provision of study materials or patients: HRK, HJP, JS, JGL, KYC, NHC, HSS, SP, GMK, HIY, HGK, YWJ, BCC, SYP, SYR, S-JH. Collection and assembly of data: HRK, HJP, JS, JGL, KYC, GMK, HIY, HGK, YWJ, BCC, SYP, SYR, S-JH. Data analysis and interpretation: HRK, HJP, SYP, SYR, S-JH. Manuscript writing: All authors. Final approval of manuscript: All authors.

Funding
This work was supported by grants from the National Research Foundation of the Republic of Korea (2018R1A2A1A05076997, 2017R1A5A1014560, 2018M3A9H3024850, and 2019M3A9B6065221 to S-J.H.; 2017M3A9E9072669, 2017M3A9E8029717, 2017R1D1A1B03029874, and 2019M3A9B6065231 to H.R.K).

Availability of data and materials
All data generated or analysed during this study are included in this published article and its supplementary information files.

Ethics approval and consent to participate
The study was approved by the Institutional Review Board of Severance Hospital. All animal protocols were approved by the Institutional Animal Care and Use Committee of the Yonsei University Laboratory Animal Research Center (2013–0115).

Consent for publication
All authors agreed with publication.

Competing interests
The authors declare that they have no competing interest that are relevant to this study.

Author details
[1]Yonsei Cancer Center, Division of Medical Oncology, Yonsei University College of Medicine, 50 Yonsei-ro, Seodaemun-Gu, Seoul 120-752, South Korea. [2]Department of Biochemistry, College of Life Science & Biotechnology, Yonsei University, Seoul, South Korea. [3]Department of Thoracic and Cardiovascular Surgery, Yonsei University College of Medicine, 50 Yonsei-ro, Seodaemun-Gu, Seoul 120-752, South Korea. [4]Department of Pathology, Yonsei University College of Medicine, Seoul, South Korea. [5]Department of Radiation Oncology, Yonsei University College of Medicine, Seoul, South Korea. [6]Department of Pharmacy, Korea University, Sejong, South Korea.

Received: 13 December 2018 Accepted: 22 October 2019
Published online: 04 December 2019

References
1. Gettinger SN, Horn L, Gandhi L, Spigel DR, Antonia SJ, Rizvi NA, et al. Overall survival and long-term safety of Nivolumab (anti-programmed death 1 antibody, BMS-936558, ONO-4538) in patients with previously treated advanced non-small-cell lung Cancer. J Clin Oncol. 2015;33(18):2004. https://doi.org/10.1200/jco.2014.58.3708.
2. Garon EB, Rizvi NA, Hui R, Leighl N, Balmanoukian AS, Eder JP, et al. Pembrolizumab for the treatment of non-small-cell lung Cancer. N Engl J Med. 2015. https://doi.org/10.1056/NEJMoa1501824.
3. Ribas A. Tumor immunotherapy directed at PD-1. N Engl J Med. 2012; 366(26):2517–9.
4. Sakuishi K, Apetoh L, Sullivan JM, Blazar BR, Kuchroo VK, Anderson AC. Targeting Tim-3 and PD-1 pathways to reverse T cell exhaustion and restore anti-tumor immunity. J Exp Med. 2010;207(10):2187–94.
5. Nishikawa H, Sakaguchi S. Regulatory T cells in tumor immunity. Int J Cancer. 2010;127(4):759–67.
6. Kurtulus S, Sakuishi K, Ngiow SF, Joller N, Tan DJ, Teng MW, et al. TIGIT predominantly regulates the immune response via regulatory T cells. J Clin Invest. 2015;125(11):4053–62.
7. Scurr MJ, Pembroke T, Bloom A, Roberts DJ, Thomson A, Smart K, et al. Low-dose cyclophosphamide induces anti-tumor T-cell responses which associate with survival in metastatic colorectal cancer. Clin Cancer Res. 2017. https://doi.org/10.1158/1078-0432.ccr-17-0895.
8. Sugiyama D, Nishikawa H, Maeda Y, Nishioka M, Tanemura A, Katayama I, et al. Anti-CCR4 mAb selectively depletes effector-type FoxP3+CD4+ regulatory T cells, evoking antitumor immune responses in humans. Proc Natl Acad Sci U S A. 2013;110(44):17945–50.
9. Park HJ, Kusnadi A, Lee EJ, Kim WW, Cho BC, Lee IJ, et al. Tumor-infiltrating regulatory T cells delineated by upregulation of PD-1 and inhibitory receptors. Cell Immunol. 2012;278(1–2):76–83.
10. Kang MJ, Kim KM, Bae JS, Park HS, Lee H, Chung MJ, et al. Tumor-infiltrating PD1-positive lymphocytes and FoxP3-positive regulatory T cells predict distant metastatic relapse and survival of clear cell renal cell carcinoma. Transl Oncol. 2013;6(3):282–9.
11. Penaloza-MacMaster P, Kamphorst AO, Wieland A, Araki K, Iyer SS, West EE, et al. Interplay between regulatory T cells and PD-1 in modulating T cell exhaustion and viral control during chronic LCMV infection. J Exp Med. 2014;211(9):1905–18.
12. Park HJ, Park JS, Jeong YH, Son J, Ban YH, Lee BH, et al. PD-1 Upregulated on regulatory T cells during chronic virus infection enhances the suppression of CD8+ T cell immune response via the interaction with PD-L1 expressed on CD8+ T cells. J Immunol. 2015;194(12):5801–11.

13. Sakuishi K, Ngiow SF, Sullivan JM, Teng MW, Kuchroo VK, Smyth MJ, et al. TIM3FOXP3 regulatory T cells are tissue-specific promoters of T-cell dysfunction in cancer. Oncoimmunology. 2013;2(4):e23849.
14. Gautron AS, Dominguez-Villar M, de Marcken M, Hafler DA. Enhanced suppressor function of TIM-3+ FoxP3+ regulatory T cells. Eur J Immunol. 2014;44(9):2703–11.
15. Wing K, Onishi Y, Prieto-Martin P, Yamaguchi T, Miyara M, Fehervari Z, et al. CTLA-4 control over Foxp3+ regulatory T cell function. Science. 2008; 322(5899):271–5.
16. Sojka DK, Hughson A, Fowell DJ. CTLA-4 is required by CD4+CD25+ Treg to control CD4+ T-cell lymphopenia-induced proliferation. Eur J Immunol. 2009;39(6):1544–51.
17. Francisco LM, Salinas VH, Brown KE, Vanguri VK, Freeman GJ, Kuchroo VK, et al. PD-L1 regulates the development, maintenance, and function of induced regulatory T cells. J Exp Med. 2009;206(13):3015–29.
18. Periasamy S, Dhiman R, Barnes PF, Paidipally P, Tvinnereim A, Bandaru A, et al. Programmed death 1 and cytokine inducible SH2-containing protein dependent expansion of regulatory T cells upon stimulation with mycobacterium tuberculosis. J Infect Dis. 2011;203(9):1256–63.
19. Wang L, Pino-Lagos K, de Vries VC, Guleria I, Sayegh MH, Noelle RJ. Programmed death 1 ligand signaling regulates the generation of adaptive Foxp3+CD4+ regulatory T cells. Proc Natl Acad Sci U S A. 2008;105(27): 9331–6.
20. Franceschini D, Paroli M, Francavilla V, Videtta M, Morrone S, Labbadia G, et al. PD-L1 negatively regulates CD4+CD25+Foxp3+ Tregs by limiting STAT-5 phosphorylation in patients chronically infected with HCV. J Clin Invest. 2009;119(3):551–64.
21. Radziewicz H, Dunham RM, Grakoui A. PD-1 tempers Tregs in chronic HCV infection. J Clin Invest. 2009;119(3):450–3.
22. Shen T, Zheng J, Liang H, Xu C, Chen X, Zhang T, et al. Characteristics and PD-1 expression of peripheral CD4+CD127loCD25hiFoxP3+ Treg cells in chronic HCV infected-patients. Virol J. 2011;8:279.
23. Lowther DE, Goods BA, Lucca LE, Lerner BA, Raddassi K, van Dijk D, et al. PD-1 marks dysfunctional regulatory T cells in malignant gliomas. JCI Insight. 2016;1(5):1.
24. Dhanji S, Tse K, Teh HS. The low affinity fc receptor for IgG functions as an effective cytolytic receptor for self-specific CD8 T cells. J Immunol. 2005; 174(3):1253–8.
25. Kudo K, Imai C, Lorenzini P, Kamiya T, Kono K, Davidoff AM, et al. T lymphocytes expressing a CD16 signaling receptor exert antibody-dependent cancer cell killing. Cancer Res. 2014;74(1):93–103.
26. Zelenay S, Lopes-Carvalho T, Caramalho I, Moraes-Fontes MF, Rebelo M, Demengeot J. Foxp3+ CD25- CD4 T cells constitute a reservoir of committed regulatory cells that regain CD25 expression upon homeostatic expansion. Proc Natl Acad Sci U S A. 2005;102(11):4091–6.
27. Kolar P, Knieke K, Hegel JK, Quandt D, Burmester GR, Hoff H, et al. CTLA-4 (CD152) controls homeostasis and suppressive capacity of regulatory T cells in mice. Arthritis Rheum. 2009;60(1):123–32.
28. Gordon SR, Maute RL, Dulken BW, Hutter G, George BM, McCracken MN, et al. PD-1 expression by tumour-associated macrophages inhibits phagocytosis and tumour immunity. Nature. 2017;545(7655):495–9.
29. Beldi-Ferchiou A, Lambert M, Dogniaux S, Vely F, Vivier E, Olive D, et al. PD-1 mediates functional exhaustion of activated NK cells in patients with Kaposi sarcoma. Oncotarget. 2016;7(45):72961–77.
30. Seo H, Jeon I, Kim BS, Park M, Bae EA. IL-21-mediated reversal of NK cell exhaustion facilitates anti-tumour immunity in MHC class I-deficient tumours. Nat Commun. 2017;8:15776.
31. Seo H, Kim BS, Bae EA, Min BS, Han YD, Shin SJ, et al. IL21 therapy combined with PD-1 and Tim-3 blockade provides enhanced NK cell antitumor activity against MHC class I-deficient tumors. Cancer Immunol Res. 2018;6(6):685–95.
32. Iraolagoitia XL, Spallanzani RG. NK Cells Restrain Spontaneous Antitumor CD8+ T Cell Priming through PD-1/PD-L1 Interactions with Dendritic Cells. J Immun. 2016;197(3):953–61.
33. Liu Y, Cheng Y, Xu Y, Wang Z, Du X, Li C, et al. Increased expression of programmed cell death protein 1 on NK cells inhibits NK-cell-mediated anti-tumor function and indicates poor prognosis in digestive cancers. Oncogene. 2017;36(44):6143–53.
34. Vari F, Arpon D, Keane C, Hertzberg MS, Talaulikar D, Jain S, et al. Immune evasion via PD-1/PD-L1 on NK cells and monocyte/macrophages is more prominent in Hodgkin lymphoma than DLBCL. Blood. 2018;131(16):1809–19.
35. Tumino N, Martini S, Munari E, Scordamaglia F, Besi F, Mariotti FR, et al. Presence of innate lymphoid cells in pleural effusions of primary and metastatic tumors: Functional analysis and expression of PD-1 receptor. Int J Cancer. 2019;145(6):1660–8.
36. Setiady YY, Coccia JA, Park PU. In vivo depletion of CD4+FOXP3+ Treg cells by the PC61 anti-CD25 monoclonal antibody is mediated by FcgammaRIII+ phagocytes. Eur J Immunol. 2010;40(3):780–6.

Publisher's Note